

Submitted: 20/06/2022

Accepted: 01/11/2022

Published: 01/12/2022

Evaluation of setup errors of immobilization device for radiation therapy in companion animals

Toshie Iseri¹ , Nanami Hira² , Yoshinori Tanabe^{3*} , Hiro Horikirizono⁴ , Hiroshi Sunahara⁴ , Harumichi Itoh⁴ , Yuki Nemoto⁴ , Kazuhito Itamoto⁴ , Kenji Tani⁴ , and Munekazu Nakaichi⁴ 

¹Faculty of Agriculture, Animal Medical Emergency Center, Tokyo University of Agriculture and Technology, Tokyo, Japan

²Faculty of Health Sciences, Okayama University Medical School, Okayama, Japan

³Faculty of Medicine, Graduate School of Health Sciences, Okayama University, Okayama, Japan

⁴Joint Faculty of Veterinary Medicine, Yamaguchi University, Yamaguchi, Japan

Abstract

Background: Intensity-modulated radiotherapy (IMRT), which allows generating steep dose gradients, is a beneficial treatment for companion animals with adjacent target and risk organs. IMRT is essential for high setup accuracy for avoiding overdose to risk organs, and optimal radiotherapy is important for evaluating the setup accuracy of companion animals.

Aim: To use an immobilization device to evaluate setup errors in radiotherapy for companion animals.

Methods: We calculated setup errors in radiotherapy for 386 animals (dogs and cats; 3,261 registration images) that underwent radiotherapy between 2016 and 2022. The companion animals were immobilized with a customized bite block and vacuum lock device. A quantile–quantile plot with 95% confidence interval (CI) was used to evaluate the histogram of the setup errors, and the systematic and random setup errors were calculated for each region (brain, head and neck, chest and abdomen, pelvis, and spine).

Results: The setup error in each direction presented an extremely narrow-interval histogram, with the following lower and upper 95% CIs: cranial–caudal (−0.08, −0.06 cm); left–right (−0.04, −0.02 cm); and dorsal–ventral (−0.13, −0.11 cm). The mean systematic setup error was 0.16 cm (range: 0.12–0.36 cm), and the random error was 0.15 cm (range: 0.08–0.34 cm). The pelvis showed the highest systematic and random setup errors (mean: 0.36 and 0.23 cm, respectively).

Conclusion: The use of an immobilization device enables highly accurate radiotherapy for companion animals (95% CI < 0.15 cm).

Keywords: Companion animals, Head and neck, Immobilization device, Radiation therapy, Setup error.

Introduction

Similar to surgical intervention and chemotherapy, radiotherapy is a critical treatment in veterinary medicine (Clerc-Renaud *et al.*, 2021). Intensity-modulated radiotherapy (IMRT) generates steep dose gradients and can deliver precise dose distributions to the target organs, thereby preventing the administration of high doses in the neighboring organs at risk (OARs) (Lawrence *et al.*, 2010). The steep dose gradient of IMRT may cause adverse effects due to the positional deviation of setup errors, and the positional deviations for target organs and OARs may lead to a difference between the planned and actual doses (Deveau *et al.*, 2010; Tanabe *et al.*, 2021). The setup error is considered the planning target volume (PTV) margin of uncertainty, and the radiotherapy dose is safely delivered to the target organ within the PTV margin

(Noghreiyani *et al.*, 2020). In human radiotherapy, the PTV margin is calculated according to a formula by Stroom *et al.* (1999) and Van Herk *et al.* (2002) using setup error; the formula considers the clinical target volume dose coverage determined by tests of realistic human plans. The setup can estimate the systematic and random setup errors during actual treatment based on the results of previous studies (Stroom *et al.*, 1999; van Herk *et al.*, 2002).

It is difficult to mark the body surface of furred animals using a paint pen for alignment and reference in planning computed tomography (CT) images, compared with the marking procedure performed on humans, and the absence of anatomical gradients in animals reduces setup accuracy and reproducibility (Freislederer *et al.*, 2020). Therefore, a more robust immobilization device is needed to maintain the setup of an animal for reproducing

*Corresponding Author: Yoshinori Tanabe. Faculty of Medicine, Graduate School of Health Sciences, Okayama University, Okayama, Japan. Email: tanabey@okayama-u.ac.jp

the animal position at the time of acquiring planning CT images; therefore, most facilities specifically customize the device for different species of animals (Tillner *et al.*, 2014). Evaluating the setup accuracy of an immobilization device specifically designed for an animal is important for determining the PTV margin, which helps reduce the dose difference between the planned and actual doses. In human medicine, the setup errors of immobilization devices have been evaluated in several studies (Suzuki *et al.*, 2012; Strbac and Jokic, 2013; Noghreiyani *et al.*, 2020), and the results can be compared with the setup accuracy of radiotherapy in veterinary medicine. To the best of our knowledge, although studies on the evaluation of head and neck setup errors have been reported in animal radiotherapy (Morimoto *et al.*, 2020), the evaluation of setup errors in each anatomical region from the head to the pelvis of the target for IMRT has not yet been elucidated. This study aimed to assess the setup accuracy in animal radiotherapy by evaluating 386 cases (brain, head and neck, chest and abdomen, pelvis, and spine). The results obtained via positioning of a surface without markers and using an immobilization device with a special bite block and vacuum lock device for animal (dog or cat) radiotherapy have potential applications in human medicine.

Materials and Methods

Subjects and devices

The subjects included 386 animals that underwent radiotherapy (brain: 108; head and neck: 235; chest

and abdomen: 3; pelvis: 21; and spine: 10) from May 2016 to December 2022. The image registration system comprised Synergy (Elekta AB, Stockholm, Sweden) as the treatment device and an electronic portal imaging device (EPID). The treatment planning system Monaco (Elekta AB, Stockholm, Sweden, ver. 5.11) was used to create a digitally reconstructed radiograph (DRR) for animal positioning during treatment. In total, 3,261 registration images were used to evaluate the setup error.

Immobilization device for animal radiotherapy

To obtain planning CT scan, an immobilization device was created, which used a special bite block made of Gee's ExaFlex Putty and a Vac-Lok™ cushion (Civco Medical Solutions, Kalona, IA) (Fig. 1). Bite blocks were created for animals with and without all teeth. As shown in Figure 1, the bite block was combined with Styrofoam™ (DuPont) with holes for the passage of the endotracheal tube for inhalation anesthesia. In the animal setup for CT scanning, a laser was used to mark Vac-Lok™ in the left–right (LR), dorsal–ventral (DV), and cranial–caudal (CC) directions using a laser in the CT room.

Calculation of setup error during treatment

The animals were positioned on the base of Vac-Lok™ at the marks for each direction for treatment, and bone matching was performed for image registration between DRR and EPID images. We used 3,261 image registration data elements for 386 cases to calculate the difference between the spatial coordinates obtained before and after bone matching (LR, DV, and CC).

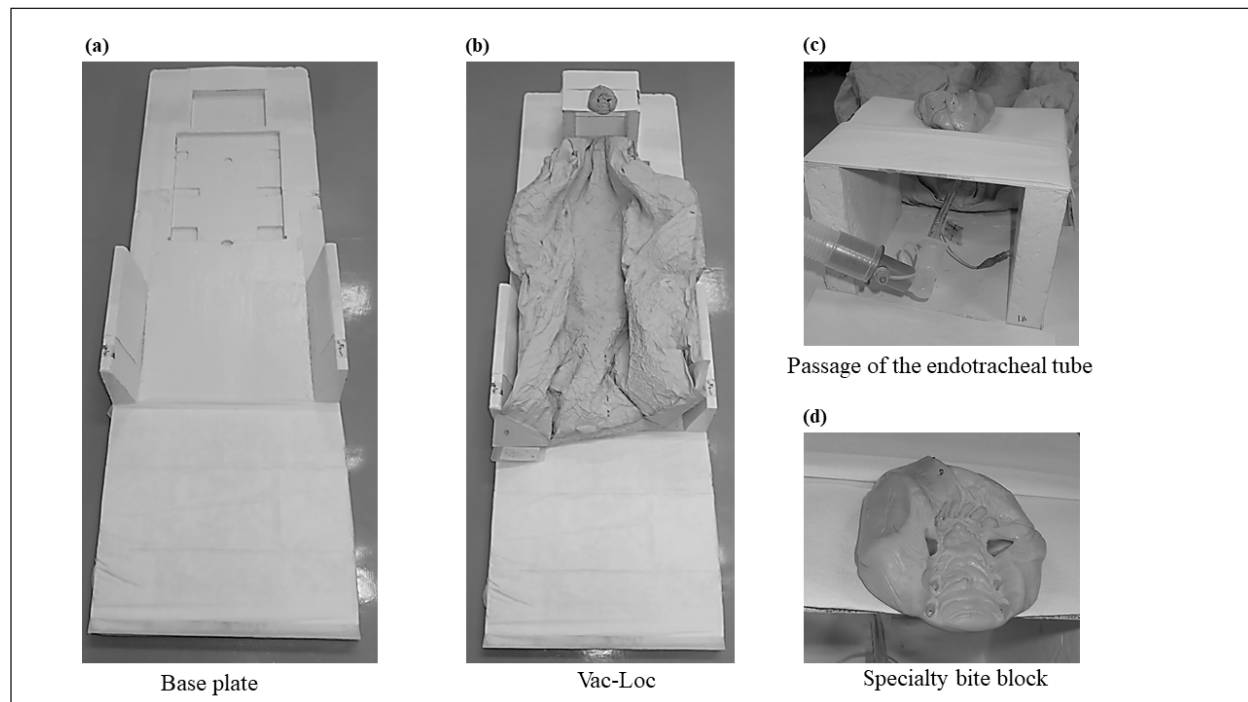


Fig. 1. An immobilization device for animal radiotherapy. (a) Base plate for immobilization device, (b) immobilization of Vac-Loc™ and bite block was combined with Styrofoam™, (c) bite block was combined with Styrofoam™ with holes to allow passage of the endotracheal tube for inhalation anesthesia, and (d) special bite block of Gee's ExaFlex Putty type.

The three-dimensional (3D) displacement error was calculated using the following formula:

$$3D \text{ displacement error} = \sqrt{LR^2 + DV^2 + CC^2} \quad (1)$$

The animal motion management of intrafraction errors during treatment was controlled using a preanesthetic medication.

Evaluation of histograms of setup errors for all cases

Each directional histogram of the setup errors for all cases was evaluated using normality, and a quantile–quantile (Q–Q) plot was constructed using JMP pro15 statistical software (SAS Inc., Cary, NC). The histograms of each directional setup error for all cases were calculated using upper and lower 95% confidence intervals (CIs) and analyzed using the Anderson–Darling normality test ($p < 0.05$).

Evaluation of setup error for each region

For the regional groups (brain, head and neck, chest and abdomen, pelvis, and spine), the average and standard deviation (SD) setup errors were calculated in each direction (LR, DV, and CC), and significant differences between each group were assessed using the Mann–Whitney *U* test ($p < 0.05$).

Subsequently, the systematic setup error (Σ) and random setup error (σ) were calculated using the setup errors of each regional group according to the following equations:

$$\Sigma = \sqrt{\frac{1}{n-1} \sum_{i=1}^n (\mu_i - \bar{\mu})^2} \quad (2)$$

$$\sigma = \sqrt{\frac{1}{n} \sum_{i=1}^n (\sigma_i)^2} \quad (3)$$

where, Σ is the mean value of the setup error for each case and σ is the SD of the setup error for each case.

Statistical analysis

The Anderson–Darling normality test predicts the hypothesis of normality at p -values of <0.05 . The statistically significant differences were assessed using the Mann–Whitney *U* test via JMP Pro version 15 statistical software. Regarding the results, the differences were considered statistically significant at p -values of <0.05 .

Ethical approval

This study did not require ethical approval as the data were retrospectively analyzed.

Results

The histograms of each directional setup error for all data are shown in Figure 2. For each direction (CC, LR, and DV), extremely narrow-interval histograms were observed, which did not show a standard normal distribution. The tail of the Q–Q plot line deviated from a straight line (Fig. 2); the largest tail spread was observed in the CC direction. Further, the all-direction data were not normally distributed in the Anderson–Darling normality test ($p < 0.05$). The lower and upper 95% CIs of the setup errors for CC, LR, and DV were (–0.08, –0.06 cm), (–0.04, –0.02 cm), and (–0.13, –0.11 cm), respectively.

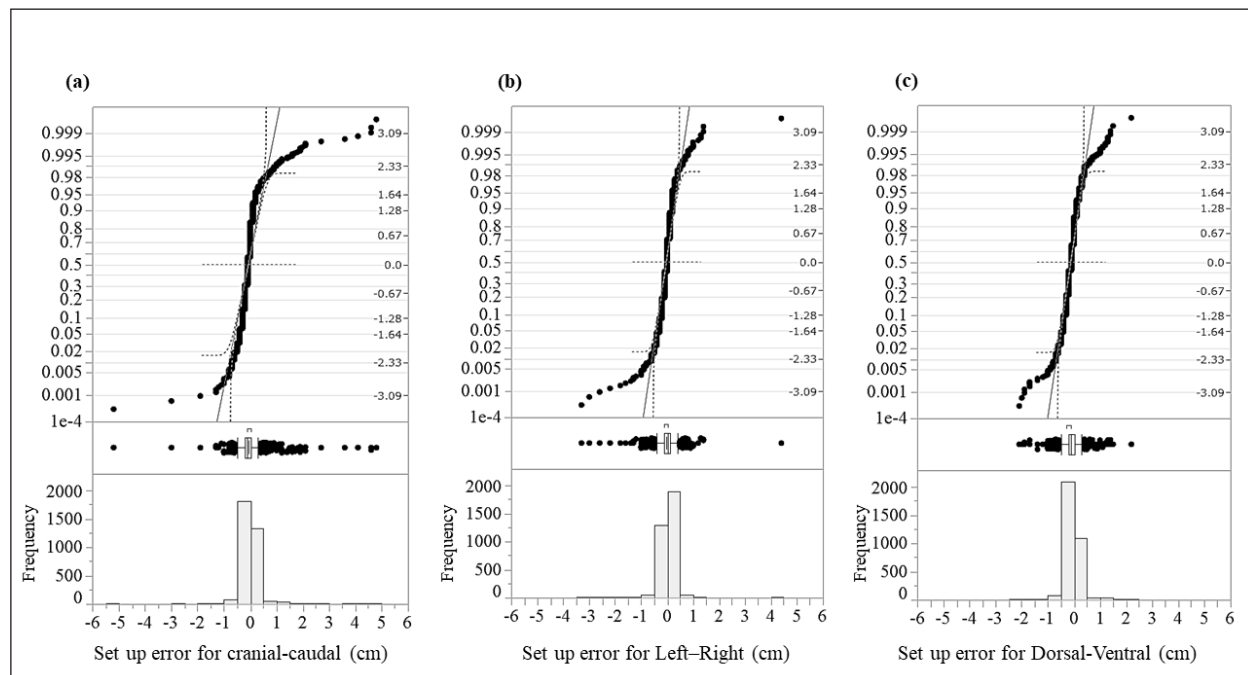


Fig. 2. Evaluation of the histograms of setup errors for all cases (upper part: normal Q–Q plot, middle part: box plot, lower part: histogram). (a) Setup error for CC direction, (b) setup error for LR direction, and (c) setup error for DV direction.

Table 1. Average and SD setup error for each direction in each regional group.

Region	Fractions; mean (min–max)	The average setup error for CC: mean (min–max) (cm)	The average setup error for LR: mean (min–max) (cm)	The average setup error for DV: mean (min–max) (cm)
		The SD for CC: mean (max) (cm)	The SD for LR: mean (min–max) (cm)	The SD for DV: mean (min–max) (cm)
Brain	10 (1–12)	–0.11 (–0.48 to 0.83)	–0.03 (–0.40 to 0.30)	–0.10 (0.40 to 0.63)
		0.10 (1.38)	0.09 (0.65)	0.10 (1.10)
Head and neck	10 (1–17)	–0.10 (–0.86 to 0.83)	–0.05 (0.54 to 0.10)	–0.20 (–0.65 to 0.46)
		0.09 (1.57)	0.10 (0.54)	0.10 (0.54)
Chest and abdomen	5 (1–12)	–0.07 (–0.34 to 0.40)	–0.16 (–0.57 to 0.03)	–0.21 (–0.70 to 0.24)
		0.23 (0.50)	0.15 (0.50)	0.18 (0.50)
Pelvis	5 (1–11)	0.00 (–0.50 to 1.12)	–0.10 (–0.58 to 0.80)	–0.18 (–0.64 to 0.22)
		0.25 (1.59)	0.25 (0.96)	0.26 (0.77)
Spine	10 (3–14)	–0.07 (–0.18 to 0.19)	–0.06 (0.05 to 0.65)	–0.11 (–0.53 to 0.28)
		0.13 (0.65)	0.15 (0.45)	0.14 (0.66)

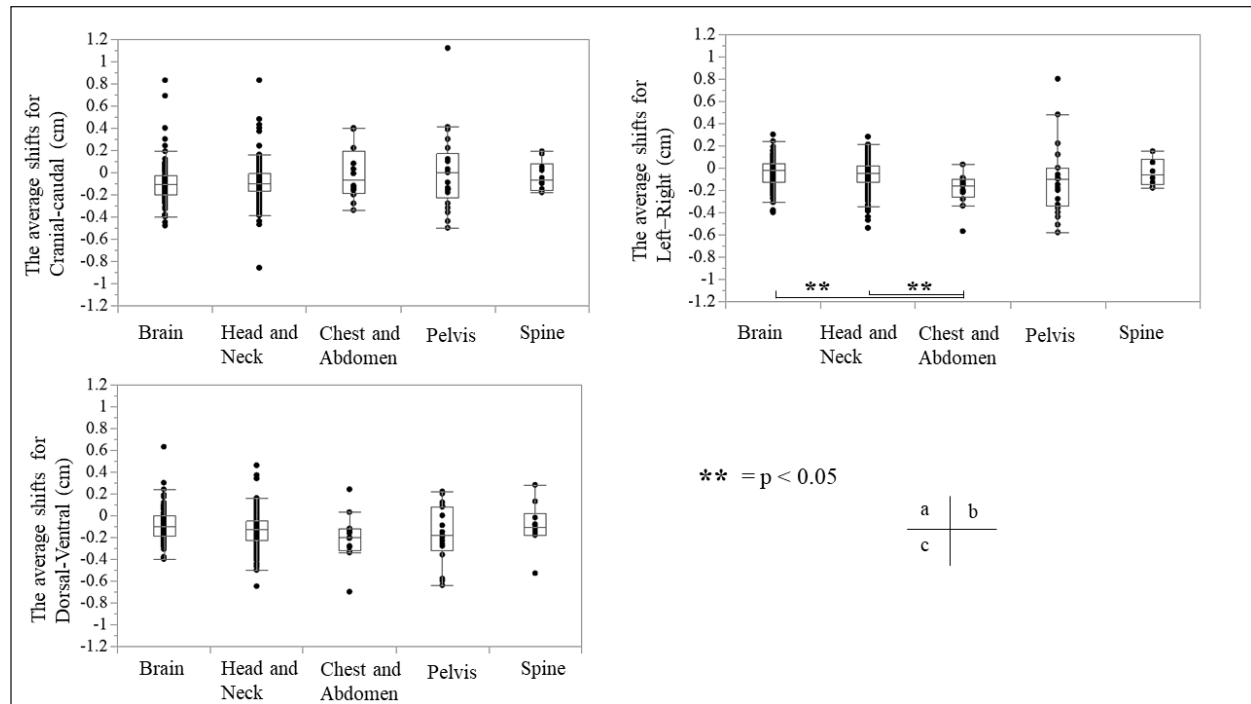


Fig. 3. Relationship between the average setup errors for each direction in each region. (a) CC direction, (b) LR direction; statistically significant differences were observed between the following: brain versus chest and abdomen, head and neck versus chest and abdomen (equal variance in Mann–Whitney *U* test; $p < 0.005$). (c) DV direction.

Table 1 and Figures 3 and 4 summarize the average and SD setup error data of the regions in each direction. The widest range of the average setup error for each region was –0.48 to 0.83 cm in the CC direction for the brain, –0.86 to 0.83 cm in the CC direction for the head and neck, –0.70 to 0.24 cm in the DV direction for the chest, –0.50 to 1.50 cm in the CC direction for the pelvis, and –0.53 to 0.28 cm in the DV direction for the spine. In each direction of the mean setup, statistically

significant differences were observed among the brain, chest and abdomen, and head and neck in the LR direction (Fig. 3b).

The SD of the setup error for each region showed statistically significant differences for the pelvis, brain, and head and neck in the CC direction, within 0.25 cm for the brain and all regions in the LR direction and within 0.26 cm for the pelvis and head and neck in the DV direction (Fig. 4).

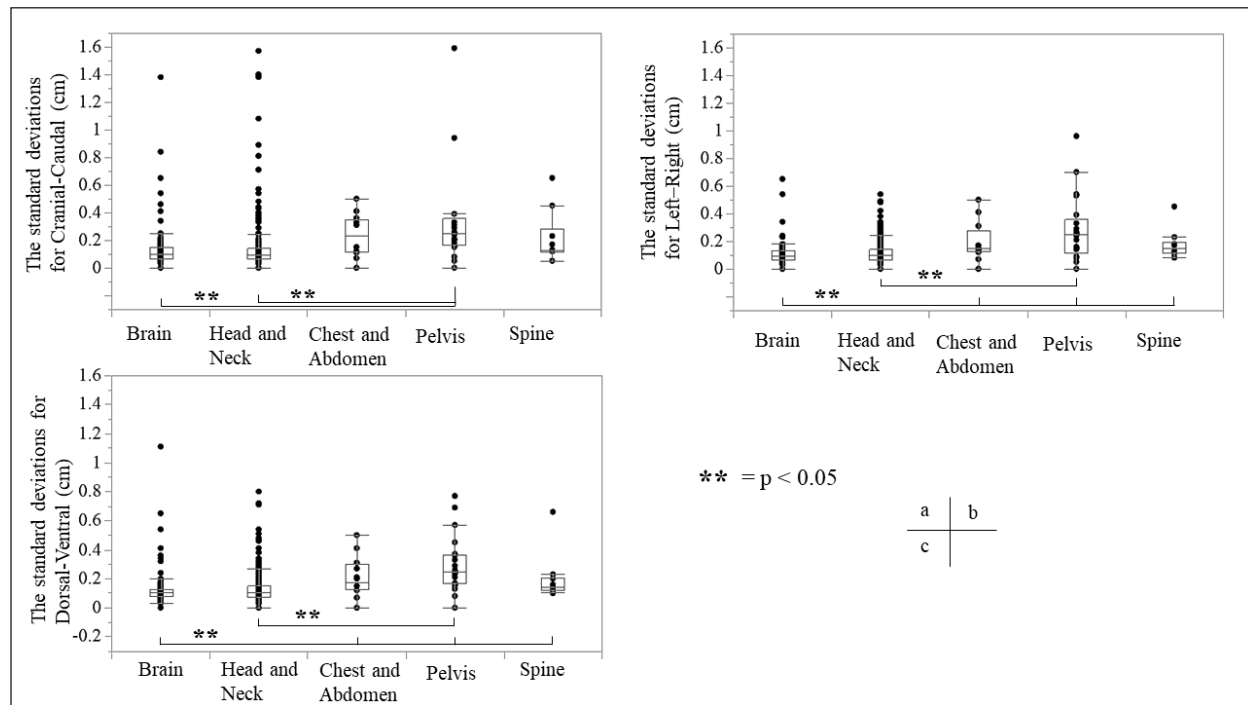


Fig. 4. Relationship between SD setup errors for each direction in each regional group. Statistically significant differences were assessed using the Mann–Whitney U test ($p < 0.005$). (a) CC direction; statistically significant differences were observed between the following: brain versus pelvis, head and neck versus pelvis. (b) LR direction; statistically significant differences were observed between the following: head and neck versus pelvis, brain versus chest and abdomen, pelvis, and spine. (c) DV direction; statistically significant differences were observed between the pelvis and the brain and head and neck. (d) LR direction; statistically significant differences were observed between the following: head and neck versus pelvis, brain versus chest and abdomen, pelvis, and spine.

Table 2. Systematic and random setup error for each direction in each regional group.

Region	CC		LR		DV	
	Σ	σ	Σ	σ	Σ	σ
Brain	0.19	0.17	0.13	0.08	0.15	0.13
Head and neck	0.16	0.20	0.13	0.08	0.15	0.11
Chest and abdomen	0.24	0.15	0.15	0.14	0.22	0.14
Pelvis	0.36	0.34	0.32	0.23	0.27	0.19
Spine	0.13	0.18	0.12	0.10	0.21	0.16

Table 2 presents the systematic and random setup errors for each region, which were <0.30 cm, except for the pelvis. The largest systematic and random setup errors were observed for the pelvis, which were Σ 0.36 cm and σ 0.34 cm in the CC direction.

Discussion

The histograms of the setup errors for all cases of animal radiotherapy showed extremely narrow intervals, with 95% CIs of ≤ 0.15 cm, which was similar to the results of the setup accuracy in human medicine (Suzuki *et al.*, 2012). Although furred animals do not have markers on their body surface, we found that the use of the immobilization device with a specialty bite block and Vac-Lock™ enabled the evaluation of high-precision animal radiotherapy.

The histograms of the setup errors did not show a standard normal distribution, and the largest tail spread of the Q–Q plot was found in the CC direction. It is considered that the tail spread of the Q–Q plot leads to decreased accuracy due to the tooth form and gingiva and the absence of anatomical gradients in animals (Freislederer *et al.*, 2020). Image-guided radiotherapy is effective in avoiding interfraction random setup errors and the influence of positioning inaccuracies (Bell *et al.*, 2018). Additionally, we believe that animal radiotherapy can more effectively control interfraction errors and tension due to the use of preanesthetic medication than human medical radiotherapy (Tanabe *et al.*, 2019).

The mean and SD of the setup error were larger in the pelvis than in other regions. Setup for the pelvis is difficult in several cases, such as for the anal sac

gland, perineum, and urethra, except for the pelvic bone. For resolving the setup of those body surfaces other than the pelvic bone, the setup error in surface-guided radiotherapy can be improved using optical surface scanning (Freislederer *et al.*, 2020). In a previous human medicine study, the systematic setup error of the pelvic bone was 0.28–0.50 cm for the setup error and 0.15–0.28 for the random setup errors using EPID image registration (Noghreiyani *et al.*, 2020). In this study, the systematic setup error of the pelvis was 0.27–0.36 cm and the random setup error was 0.19–0.34; thus, we considered the setup accuracy of animal radiotherapy to be equivalent to that of human medical radiotherapy.

First, a limitation of this study was that our method cannot be used for target matching using a 3D image registration device, such as cone-beam CT. However, the study results indicated that the setup error can be controlled to achieve accuracy in veterinary medicine similar to that in previous human medicine studies that used EPID (Noghreiyani *et al.*, 2020). Second, we could not evaluate the PTV margin using the formula used in human medicine by Stroom *et al.* (1999) and Van Herk *et al.* (2002). The systematic and random setup errors of EPID are used to calculate the PTV margin according to this formula. However, we could not determine whether the formula is appropriate for dogs and cats because of their different body shapes. Although we could evaluate the setup error in this study, we could not evaluate the PTV margin. Therefore, in the future, we may need a novel formula for calculating the optimal PTV margin for veterinary medicine based on the dose evaluation using cone-beam CT and optical surface scanning.

We evaluated the setup of each region (brain, head and neck, chest and abdomen, pelvis, and spine) in animal radiotherapy and found that the setup error could be controlled using a customized immobilization device, the use of which enabled high accuracy in animal radiotherapy. A research limitation was that we could not evaluate the PTV margin using the formula used in human medicine.

Acknowledgments

None.

Conflict of interest

The authors declare that they have no conflict of interest.

Author contributions

T.I., N.H., Y.T., and M.N. were involved in the study design and data interpretation. T.I., N.H., Y.T., H.H., H.S., H.I., Y.N., K.I., and K.T. were involved in data analysis. All authors critically revised the report, commented on the drafts of the manuscript, and approved the final report.

Funding

This publication was prepared without any external source of funding.

References

- Bell, K., Licht, N., Rube, C. and Dzierma, Y. 2018. Image guidance and positioning accuracy in clinical practice: influence of positioning errors and imaging dose on the real dose distribution for head and neck cancer treatment. *Radiat. Oncol.* 13, 190.
- Clerc-Renaud, B., Gieger, T.L., LaRue, S.M. and Nolan, M.W. 2021. Treatment of genitourinary carcinoma in dogs using nonsteroidal anti-inflammatory drugs, mitoxantrone, and radiation therapy: a retrospective study. *J. Vet. Intern. Med.* 35, 1052–1061.
- Deveau, M.A., Gutiérrez, A.N., Mackie, T.R., Tomé, W.A. and Forrest, L.J. 2010. Dosimetric impact of daily setup variations during treatment of canine nasal tumors using intensity-modulated radiation therapy. *Vet. Radiol. Ultrasound.* 51, 90–96.
- Freislederer, P., Kügele, M., Öllers, M., Swinnen, A., Sauer, T.O., Bert, C., Giantsoudi, D., Corradini, S. and Batista, V. 2020. Recent advanced in surface guided radiation therapy. *Radiat. Oncol.* 15, 187.
- Lawrence, J.A., Forrest, L.J., Turek, M.M., Miller, P.E., Mackie, T.R., Jaradat, H.A., Vail, D.M., Dubielzig, R.R., Chappell, R. and Mehta, M.P. 2010. Proof of principle of ocular sparing in dogs with sinonasal tumors treated with intensity-modulated radiation therapy. *Vet. Radiol. Ultrasound.* 51, 561–570.
- Morimoto, C.Y., Mayer, M.N., Sidhu, N., Bloomfield, R. and Waldner, C.L. 2020. Setup error with and without imageguidance using two canine intracranial positioning systems for radiation therapy. *Vet. Comp. Oncol.* 18, 607–614.
- Noghreiyani, V.V., Nasser, S., Anvari, K., Naji, M. and Momenzad, M. 2020. Evaluation of set-up errors and determination of set-up margin in pelvic radiotherapy by electronic portal imaging device (EPID). *J. Radiother. Pract.* 19, 150–156.
- Strbac, B. and Jokic, V.S. 2013. Evaluation of set-up errors in head and neck radiotherapy using electronic portal imaging. *Phys. Med.* 29, 531–536.
- Stroom, J.C., de Boer, H.C., Huizenga, H. and Visser, A.G. 1999. Inclusion of geometrical uncertainties in radiotherapy treatment planning by means of coverage probability. *Int. J. Radiat. Oncol. Biol. Phys.* 43, 905–919.
- Suzuki, J., Tateoka, K., Shima, K., Yaegashi, Y., Fujimoto, K., Saitoh, Y., Nakata, A., Abe, T., Nakazawa, T., Sakata, K. and Hareyama, M. 2012. Uncertainty in patient set-up margin analysis in radiation therapy. *J. Radiat. Res.* 53, 615–619.
- Tanabe, Y., Ishida, T., Eto, H., Sera, T., Emoto, Y. and Shimokawa, M. 2021. Patient-specific radiotherapy quality assurance for estimating actual treatment dose. *Med. Dosim.* 46, e5–e10.
- Tanabe, Y., Ishida, T., Eto, H., Sera, T. and Emoto, Y. 2019. Evaluation of the correlation between pro static displacement and rectal deformation using the Dice similarity coefficient of the rectum. *Med. Dosim.* 44, e39–e43.

Tillner, F., Thute, P., Bütof, R., Krause, M. and Enghardt, W. 2014. Pre-clinical research in small animals using radiotherapy technology—a bidirectional translational approach. *Z. Med. Phys.* 24, 335–351.

van Herk, M., Remeijer, P. and Lebesque, J.V. 2002. Inclusion of geometric uncertainties in treatment plan evaluation. *Int. J. Radiat. Oncol. Biol. Phys.* 52, 1407–1422.